

# **NANOTECHNOLOGY FOR WATER PURIFICATION**



# NANOTECHNOLOGY FOR WATER PURIFICATION

*Edited by*  
Tania Dey



BrownWalker Press  
Boca Raton

*Nanotechnology for Water Purification*

Copyright © 2012 Tania Dey

All rights reserved. No part of this book may be reproduced or transmitted in any form or by any means, electronic or mechanical, including photocopying, recording, or by any information storage and retrieval system, without written permission from the publisher.

BrownWalker Press  
Boca Raton, Florida  
USA • 2012

ISBN-10: 1-61233-619-1  
ISBN-13: 978-1-61233-619-0

[www.brownwalker.com](http://www.brownwalker.com)

Cover image @Cutcaster.com/Elena Elisseeva

Library of Congress Cataloging-in-Publication Data

Nanotechnology for water purification / edited by Tania Dey.

pages cm

Includes bibliographical references and index.

ISBN 978-1-61233-619-0 (pbk. : alk. paper) -- ISBN 1-61233-619-1 (pbk. : alk. paper)

1. Water--Purification--Materials. 2. Water--Purification--Equipment and supplies. 3. Nanostructured materials--Industrial applications. I. Dey, Tania, 1973- editor of compilation.

TD430.N276 2012

628.1'6--dc23

2012040198

*This book is dedicated to my beloved parents  
and to the scientists who have a passion for the environment.*



## PREFACE

One of the most serious problems affecting humanity is the lack of water resources for human consumption. Worldwide 1.2 billion people do not have access to clean and safe drinking water and 2.4 billion people lack sanitation. Every year 5 million people die of waterborne diseases (World Health Organization, WHO). This situation is particularly dramatic in the least developed regions of Asia, Central and South America and Africa, where new water treatment processes are needed urgently. Problems with water are expected to grow worse in the coming decades, with water scarcity occurring globally, even in regions currently considered water-rich. Addressing these problems calls out for a tremendous amount of research to be conducted to identify new technologies for purifying water at lower cost and with less energy, while at the same time minimizing the use of chemicals and impact on the environment.

Nanotechnology has been identified as a technology that could play an important role in resolving many of the problems related to water purification and water quality. Nanomaterials and nanostructures have nano-scale dimensions in the range of 1 to 100 nm and often exhibit novel and significantly changed physical, chemical and biological properties. This is due to their structure, larger surface area per unit of volume and quantum effects that occur at the nano-scale.

Nanotechnology is a highly inter- and multi- disciplinary application oriented research area. Not only does it find its use in nanomedicine, solar cells, sensor development and so on, but can also be effectively utilized to prevent water pollution. Nanostructured materials such as magnetic nanoparticles, carbon nanotubes, silver-impregnated cyclodextrin nanocomposites, nanostructured iron-zeolites, carbo-iron nanomaterials, photocatalytic titania nanoparticles, nanofiltration membranes and functionalized silica nanoparticles can be employed in water treatment – to remove heavy metals, sediments, chemical effluents, charged particles, bacteria and other pathogens. This edited book comprises several review-style chapters written by world experts. The chapters are devoted to each of these nanotechnology based approaches: basic principles, practical applications, recent break-through and limitations associated with it. The last chapter covers the environmental risks of applying engineered nanomaterials for water purification. I hope the wealth of information and insight offered in this book will be appealing to scientists and researchers over a wide range of disciplines.

Tania Dey, PhD  
Editor, Nanotechnology for Water Purification  
Email: taniadey@hotmail.com





# CONTENTS

## Chapter 1

Magnetic Nanoparticles and Cellulosic Nanofibers to Remove Arsenic and Other Heavy Metals from Water

*Tania Dey*..... 1

## Chapter 2

Potential of Carbon Nano-Tubes (CNTs) in Desalination and Water Purification

*Soumitra Kar & P.K. Tewari*..... 29

## Chapter 3

Silver-impregnated Cylcodextrin Nanocomposite for Safe Drinking Water

*Rui W. M. Krause, Lungile N. Thwala, & Tania Dey*..... 51

## Chapter 4

Nanostructured Fe-Zeolite and Orthoferrite Nanoparticles: Fenton-like Heterogenous Catalysts for Oxidation of Water Contaminants

*Anett Georgi, Klara Rusevova, Rafael Gonzalez-Olmos, & Katrin Mackenzie*..... 71

## Chapter 5

In-situ generation of Sorption and Reaction Barriers using Colloidal Sorbents and Sorbent-carried Nano-iron

*Katrin Mackenzie, Steffen Bleyl, Ariette Schierz, & Anett Georgi*..... 89

## Chapter 6

Photocatalytic Degradation of Poorly Biodegradable Water Pollutants using Titania (TiO<sub>2</sub>) Nanoparticles

*Lucas Reijnders*..... 117

## Chapter 7

Photocatalytic Water Treatment with TiO<sub>2</sub> Nanoparticle

*Klara Hernadi, Andras Dombi, Gabor Vereb, Zsolt Pap, Akos Kmetyko, Hossam El Nazer, & Károly Mogyorósi*..... 125

## Chapter 8

Trace Organic Contaminant removal by NF/RO: Influence of Solute and Membrane Properties, Implications of Fouling and Potential of Novel Membranes

*Arne Verliefde, Arcadio Sotto Diaz, Jeonghwan Kim, & Bart van der Bruggen*..... 179

## Chapter 9

Synthesis and Application of Surface engineered Silica (SES) for Water Pollutant Removal

*Peter Majewski*..... 209

## Chapter 10

Ecological Risk Assessment of Engineered Nanoparticles used in Water Treatment

*Victor Wepener & Lungile P. Lukebele*..... 235



## I

# Magnetic Nanoparticles and Cellulosic Nanofibers to Remove Arsenic and Other Heavy Metals from Water

Tania Dey

*Brussels University, Belgium. E-mail: taniadey@hotmail.com*

1. Introduction
2. Heavy Metal pollutants in Water
3. Magnetic Nanoparticles
  - 3.1. Natural Occurrence
  - 3.2. Synthetic Approaches
    - 3.2.1. Solution Methods
      - 3.2.1.1. Co-precipitation
      - 3.2.1.2. Microemulsion
      - 3.2.1.3. Polyols
      - 3.2.1.4. High temperature decomposition of precursors
      - 3.2.1.5. Other solution techniques
    - 3.2.2. Aerosol and Vapor Methods
      - 3.2.2.1. Spray pyrolysis
      - 3.2.2.2. Laser pyrolysis
4. Cellulosic Nanofibers
  - 4.1. Natural Occurrence
  - 4.2. Processing Techniques
    - 4.2.1. Mechanical fibrillation
    - 4.2.2. Electrospinning
    - 4.2.3. Swelled precursor
    - 4.2.4. Acid hydrolysis
    - 4.2.5. By bacteria
5. State-of-Art Applications
  - 5.1. Magnetite ( $\text{Fe}_3\text{O}_4$ )
  - 5.2. Maghemite ( $\text{Fe}_2\text{O}_3$ )
  - 5.3. Nano zero valent iron (nZVI)
  - 5.4. Mixed oxides
  - 5.5. Organic-inorganic nanohybrids
  - 5.6. Cellulosic biomass
6. Nanotechnological Principal applied to Water Purification
  - 6.1. Nano effect
  - 6.2. Effect of pH
  - 6.3. Effect of competing species
  - 6.4. Effect of temperature
  - 6.5. Effect of pollutant (adsorbate) concentration
  - 6.6. Effect of contact time
  - 6.7. Effect of adsorbent dose

- 7. Limitations
- 8. Conclusion
- References

## 1. Introduction

One of the most serious problems affecting humanity is the lack of water resources for human consumption. Worldwide 1.2 billion people do not have access to clean and safe drinking water and 2.4 billion people lack sanitation [1]. Every year 5 million people die of waterborne diseases. This situation is particularly dramatic in the least developed regions of Asia, Central and South America and Africa, where new water treatment processes are needed urgently. Problems with water are expected to grow worse in the coming decades, with water scarcity occurring globally, even in regions currently considered water-rich. Addressing these problems calls out for a tremendous amount of research to be conducted to identify new technologies for purifying water at lower cost and with less energy, while at the same time minimizing the use of chemicals and impact on the environment. This review chapter highlights some of the state-of-art methodologies of using nanomaterials as adsorbents for low-cost water treatment.

Ground water contamination by heavy metals is a key environmental concern in areas where the water supply system draws primarily on groundwater. Several methods of arsenic and chromium removal are already available including oxidation-precipitation, coagulation-precipitation, electrochemical reduction, adsorption, ion exchange, solvent extraction, nano filtration and reverse osmosis [2,3]. Adsorption of arsenic and chromium on different sorbents such as iron, iron oxide, iron coated sand, iron coated activated carbon [4], and granular ferric hydroxides [5] have also been investigated. However, their use is limited due to high operation cost, sludge formation, and technical difficulties in preparation of materials.

Nanoparticles are often associated with greater reactivity due to their large surface area and unique optical, electronic, magnetic properties in comparison to bulk, originating from quantum confinement effect. Magnetic nanoparticles, especially the naturally occurring ones, such as magnetite, maghemite, zero valent iron, mixed oxides (Co-ferrites, Ni-ferrites etc) as well as cellulosic nanofibers can be used as an effective adsorbent for water remediation, making the process cost-effective and sustainable. Being a dispersed system, these adsorbents eliminate the need of high pressure streams for water purification.

## 2. Heavy Metal Pollutants in Water

Most environmental arsenic problems are the result of mobilization under natural conditions. This includes mobilization by natural weathering reactions, biological activity, geochemical reactions, volcanic emissions and other anthropogenic activities. Soil erosion and leaching contribute to  $612 \times 10^8$  and  $2380 \times 10^8$  g/year of arsenic, respectively, in dissolved and suspended forms in the oceans [6]. However, mining activities, combustion of fossil fuels, use of arsenic pesticides, herbicides, and crop desiccants and use of arsenic additives to livestock feed create additional impacts.

Higher levels of arsenic tend to be found more in ground water sources than in surface water sources of drinking water. Two forms are common in natural waters: arsenite ( $\text{AsO}_3^{3-}$ ) and arsenate ( $\text{AsO}_4^{3-}$ ), referred to as arsenic(III) and arsenic(V). Pentavalent (+5) or arsenate species are  $\text{AsO}_4^{3-}$ ,  $\text{HAsO}_4^{2-}$ ,  $\text{H}_2\text{AsO}_4^-$  while trivalent (+3) arsenites include  $\text{As}(\text{OH})_3$ ,  $\text{As}(\text{OH})_4^-$ ,  $\text{AsO}_2\text{OH}^{2-}$  and  $\text{AsO}_3^{3-}$ . Pentavalent species predominate and are stable in oxygen rich aerobic environments, whereas trivalent arsenites predominate in moderately reducing anaerobic environments such as groundwater [7].

Arsenic-contaminated water has been a serious problem especially in Vietnam, Bangladesh and some areas in the world [8,9]. These areas include Taiwan (1.82 mg/L), Hungary (0.1 mg/L), India (0.05 mg/L), Mexico (0.4 mg/L), and the southwest United States (0.1 mg/L) [10] and to some extent Argentina, Poland, Japan and New Zealand. Human exposure to arsenic can cause both short and long term health effects. Short or acute effects can occur within hours or days of exposure. Long or chronic effects occur over many years. Long term exposure to arsenic has been linked to cancer of the bladder, lungs, skin, kidneys, nasal passages, liver and prostate, as well as pigmentation changes, skin thickening (hyperkeratosis), neurological disorders, muscular weakness, loss of appetite, and nausea [11-14]. Short term exposure to high doses of arsenic can cause other adverse health effects [15, 16].

The World Health Organization (WHO) has revised the guideline for maximum permissible concentration (MPC) value of arsenic in drinking water from 50 to 10 ppb i.e. 0.05 to 0.01 mg/L [6]. However, many countries have retained the earlier WHO guideline of 50 ppb.

Another prominent heavy metal pollutant in water resources is chromium. Chromium, which is one of the most toxic metals, is mixed into river water and ground water through the electroplating industries, metal finishing, leather tanning and chrome preparations. In the United States, it is the second most common inorganic contaminant in waters after lead [17]. Chromium exists mostly in two valence states, namely Cr (III) and Cr (VI), out of which the later one is of the great concern due to its toxicity. It is a US EPA classified group A carcinogen based on its chronic effects [18]. The mechanistic cytotoxicity of Cr (VI) is not completely understood, however, a large number of studies have demonstrated that it induces oxidative stress, DNA damage and apoptotic cell death [19]. Cr (VI) has been reported to be responsible for lung cancer, chrome ulcer, perforation of nasal septum and brain and kidney damage [20]. The major cause of its acute toxicity is its rapid diffusivity through the skin which enables it to react with biological systems and damage various organs.

### 3. Magnetic Nanoparticles

#### 3.1. *Natural Occurrence*

While man strives to synthesize and utilize advanced nanomaterials, Nature's own laboratory has produced a range of highly selective nanomaterials, since ages.

Magnetite ( $\text{Fe}_3\text{O}_4$ ) is a ferrimagnetic mineral and a member of the spinel group. Magnetite is the most magnetic naturally occurring minerals on Earth [21]. Small grains of magnetite occur in almost all igneous and metamorphic rocks. Magnetite also occurs in many sedimentary rocks, including banded iron formations. In many igneous rocks, magnetite-rich and ilmenite-rich grains occur, which were precipitated together from magma. Magnetite also is produced from peridotites and dunites by serpentinization. Magnetite is sometimes found in large quantities in beach sand. Such black sands (mineral sands or iron sands) are found in various places, such as California and the west coast of New Zealand. Continuous wetting of steel surfaces results in the formation of magnetite as the main constituent of rust formed.

The mineral Hematite ( $\text{Fe}_2\text{O}_3$ ) is known to form pseudomorphs over Magnetite. However, they differ from Magnetite in that they are only weakly attracted to magnetic field and have a reddish-brown streak.

Zero Valent Iron (ZVI) is also abundant in nature, from which nanoscale Zero Valent Iron (nZVI) can be made just by milling. Li et al. has proposed a core-shell model for nZVI particle [22], where the core remains ZVI and the shell, which forms as a result of oxidation reaction, is largely

composed of iron oxides and hydroxides. It is the mixed oxide shell ( $\text{Fe}^{2+}$  and  $\text{Fe}^{3+}$ ) that provides sites for adsorption (Figure 1).

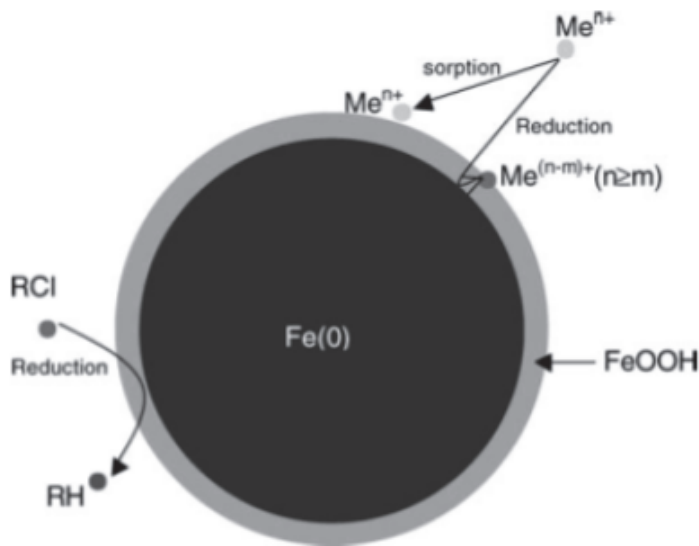


Figure 1: Core-shell model of nZVI particle, ref: [22]. Reprinted by permission of the publisher, Taylor & Francis Ltd. <http://www.tandf.co.uk/journals>

### 3.2. Synthetic Approaches

#### 3.2.1. Solution Methods

Uniform nanoparticles are usually prepared via the homogeneous precipitation reaction, a process that involves separation between nucleation and the growth of nuclei [23]. In homogeneous precipitation, a short single burst of nucleation occurs when the concentration of the constituent species reaches critical supersaturation. The nuclei so obtained are allowed to grow uniformly by diffusion of solutes from solution to surface until the final size is attained. To achieve monodispersity, these two stages must be separated, and nucleation should be avoided during the growth of nuclei. This classical model was first proposed by LaMer and Dinegar [24] to explain the mechanism of sulfur colloid formation. However, uniform particles have also been obtained after multiple nucleation events. The uniformity of the final product in this case is achieved through a self-sharpening growth process (Ostwald ripening) [25]. In addition, uniform particles have also been obtained as a result of aggregation of much smaller subunits rather than continuous growth by diffusion [26-28]. An artificial separation between nucleation and growth processes may be achieved by seeding in which foreign particles are introduced into a solution below critical supersaturation [23].

**3.2.1.1. Co-precipitation** There are mainly two methods for synthesis of spherical magnetite nanoparticles by this method. In the first, ferrous hydroxide  $\text{Fe}(\text{OH})_2$  suspensions are partially oxidized with different oxidizing agents [28]. For example, a narrow size distribution of 30-100 nm can be obtained using a  $\text{Fe}(\text{II})$  salt, a base, and a mild oxidant (like nitrate ions) [28]. The other method involves

co-precipitation of a stoichiometric mixture of ferric and ferrous hydroxides in aqueous media, yielding spherical magnetite nanoparticles of quite homogeneous size distribution [29]. In addition, it has been shown that by adjusting pH and ionic strength, it is possible to control the mean size of the nanoparticles over an order of magnitude (from 2 to 15 nm) [30]. The size decreases as the pH and ionic strength of the medium increase [30]. Both parameters affect the chemical composition of the surface and consequently the electrostatic surface charge of the particles.

**3.2.1.2. Microemulsion** Water-in-oil (w/o) microemulsions (i.e. reverse-micelle solutions) are transparent, isotropic, thermodynamically stable liquid media. In these systems, fine microdroplets of the aqueous phase are trapped within assemblies of surfactant molecules dispersed in a continuous oil phase. The surfactant-stabilized microcavities (typically in the range of 10 nm) provide a confinement effect that limits particle nucleation, growth, and agglomeration [31]. W/o microemulsions have proven to be an adequate, versatile, and simple method to prepare nanosized particles [32–37] and useful for in vivo and in vitro applications.

Pileni and coworkers [38] prepared nanosized magnetic particles with average sizes from 4 to 12 nm and a standard deviation ranging from 0.2 to 0.3 using microemulsions. A micellar solution of ferrous dodecyl sulfate  $\text{Fe}(\text{DS})_2$  was used to produce magnetic nanoparticles whose size was controlled by the surfactant concentration and temperature.

A typical transmission electron microscopy (TEM) micrograph of magnetic nanoparticles produced by this method is shown in Figure 2a. Magnetite nanoparticles of  $\sim 4$  nm in diameter have been prepared by controlled hydrolysis with ammonium hydroxide of  $\text{FeCl}_2$  and  $\text{FeCl}_3$  aqueous solutions within the reverse-micelle microcavities generated by cosurfactant AOT and heptane as a continuous oil phase [39].

Carpenter and coworkers [40] prepared metallic iron particles coated by a thin layer of gold via the microemulsion method. The gold shell not only protects the iron core but also serves as an easy means of attaching functionalities using well-known gold–thiol covalent linkage, hence making the composites lucrative for various applications. The reverse-micelle reaction is carried out using cetyltrimethylammonium bromide (CTAB) as surfactant, octane as oil phase, and aqueous reactants as water phase [41]. The metal particles are formed inside the reverse micelle by reduction of a metal salt using sodium borohydride. The synthesis technique offered by reverse micelles is sequentially applied, first to prepare the iron core by reduction of ferrous sulfate using sodium borohydride. After the reaction was allowed to reach completion, the micelles within the reaction system were enlarged to accommodate the shell using larger micelles obtained from additional borohydride. The gold shell was formed from hydrogen tetrachloroaurate solution.

Although reverse micelles have been successfully used as nanoreactors for the synthesis of magnetic nanoparticles, the main drawbacks associated with this process are (1) extensive agglomeration, (2) poor crystallinity (as the reaction is performed at relatively low temperature), and (3) low yield. However, Hyeon and coworkers [42] have reported large-scale synthesis of uniformly sized highly crystalline magnetic nanoparticles (magnetite as well as mixed metal ferrites, where metal = cobalt, manganese, nickel, and zinc), in microemulsion nanoreactors at high temperature. They have achieved good control over particle sizes from 2 to 10 nm by varying relative concentrations of precursor salt, surfactant, solvent, and the w ratio (where  $w = [\text{a polar solvent such as ethanol, methanol, or water}]/[\text{surfactant}]$ ). They have also discussed the temperature and field dependence of magnetic properties in the same paper. A similar size selection procedure in the range of 15–150 nm for  $\text{CoFe}_2\text{O}_4$  has been reported by Döker *et al.* [43]. They observed that particle size of  $\text{CoFe}_2\text{O}_4$  increases with increase in reaction time and decrease in  $\text{FeSO}_4$  percentage and AOT (the surfactant) concentration.

**3.2.1.3. Polyols** A very promising technique for the preparation of uniform nanoparticles is the polyol process. Fine metallic particles can be obtained by reduction of dissolved metallic salts and direct metal precipitation from a solution containing a polyol [44, 23]. This process was first used to prepare noble metals such as Ru, Pd, Pt, and Au and others such as Co, Ni, and Cu [45, 46]. Later the process was extended to synthesize other materials such as Fe-based alloys [47,48].

In the polyol process, the liquid polyol acts as a solvent for the metallic precursor, as well as a reducing agent and in some cases as a chelating ligand. The metal glycol can be highly or only slightly soluble in the polyol. The solution is stirred and heated to a given temperature reaching the boiling point of the polyol. By controlling the kinetics of precipitation, non-agglomerated nanoparticles of well-defined size and shape can be obtained. A better control of the average size can be achieved by seeding the reactive medium with foreign particles (heterogeneous nucleation). In this way, nucleation and growth steps can be completely separated and uniform particles can be prepared. Iron particles of  $\sim 100$  nm can be obtained by disproportionation of ferrous hydroxide in organic media [49]. Fe (II) chloride and sodium hydroxide react with ethylene glycol (EG) or polyethylene glycol, and the precipitation occurs at a temperature of  $80\text{--}100^\circ\text{C}$ .

The author of this book chapter, Dey [50, 51], has carried out some pioneering work in this area using a mixture of Fe (II) and Fe (III) chloride salts in the presence of sodium hydroxide in diethylene glycol (DEG) medium at an elevated temperature ( $210\text{--}220^\circ\text{C}$ ) under argon protection, yielding magnetite nanoparticles of very narrow size distribution and a mean diameter of  $5.6$  nm (Figure 2b). The underlying mechanism may involve three consecutive steps, such as a metal complexation reaction between hydrated metal chloride and DEG (where DEG acts as a chelating agent as well as a solvent and  $M = \text{Fe}^{2+}$ ,  $\text{Fe}^{3+}$ ,  $\text{Mn}^{2+}$ ,  $\text{Co}^{2+}$ ,  $\text{Ni}^{2+}$ , and  $\text{Zn}^{2+}$ ), followed by hydrolysis to corresponding transition metal hydroxide and finally dehydration due to heat treatment forming spinel structured metal ferrites. Capping ligands such as long-chain carboxylic acids (namely, oleic acid) were found to be quite effective in stabilizing the nanoparticles.

Furthermore, iron alloys can be obtained in a similar manner by co-precipitation of Fe, Ni, and/or Co in EG or PEG. Monodispersed quasi-spherical and nonagglomerated metallic particles with  $\sim 100$  nm diameter have been obtained without seeding, while particles between  $50$  and  $100$  nm were obtained using Pt as a nucleating agent. Whereas FeCo particles are formed by agglomerates of Fe and Co primary particles produced over different periods of time, spherical FeNi particles present good homogeneity due to concomitant Fe and Ni formation and growth by aggregation of nanometer-sized primary particles [48].

**3.2.1.4. High-temperature decomposition of precursor** The decomposition of iron precursors in the presence of hot organic surfactant has yielded markedly improved samples with good size control, narrow size distribution, and good crystallinity of well-dispersed iron oxide nanoparticles. For example, Alivisatos and coworkers [52] have demonstrated that injecting solutions of  $\text{FeCup}_3$  ( $\text{Cup} = \text{N-nitrosophenylhydroxylamine}$ ) in octylamine into long-chain amines at  $250\text{--}300^\circ\text{C}$  yields nanocrystals of maghemite. These nanocrystals range from  $4$  to  $10$  nm in diameter, are crystalline, and are dispersible in organic solvents. Hyeon and coworkers [53] have also been able to prepare monodisperse maghemite nanoparticles by a nonhydrolytic synthetic method. For example, to prepare maghemite nanoparticles of  $13$  nm diameter (Figure 2c),  $\text{Fe}(\text{CO})_5$  was injected into a solution containing surfactant and a mild oxidant (trimethylamine oxide).

Recently, Sun and Zeng [54] have been able to prepare monodispersed magnetite nanoparticles with sizes from  $3$  to  $20$  nm by high-temperature ( $265^\circ\text{C}$ ) reaction of iron(III) acetylacetonate with phenyl ether in the presence of alcohol, oleic acid, and oleylamine. In particular, magnetite nanoparti-



cles of size  $\sim 4$  nm were obtained by thermal decomposition of the iron precursor, although to obtain diameters up to 20 nm seed-mediated growth was required.

Varma and coworkers [55] have synthesized iron oxide nanoparticles in three major phases – namely,  $\alpha$ - and  $\gamma$ -Fe<sub>2</sub>O<sub>3</sub> and Fe<sub>3</sub>O<sub>4</sub> – by a self-sustained solution combustion approach and by using a range of precursors and oxidizers such as iron nitrate and oxalate, as well as different fuels (e.g., glycine and hydrazine). The product was found to have good crystalline structure and surface area in the range 50–175 m<sup>2</sup>/g, avoiding the need of additional calcination procedures. They showed how the product composition and properties can be controlled by varying oxidizer as well as fuel.

**3.2.1.5. Other solution techniques** Sonochemistry-assisted synthesis has also been reported as an adequate method for the production of magnetite and maghemite nanoparticles [56–58]. In sonochemistry, the acoustic cavitation (i.e., the formation, growth, and implosive collapse of a bubble in an irradiated liquid) generates a transient localized spot, with an effective temperature of 5000 K and a nanosecond lifetime [59]. The cavitation is a quenching process, and hence the composition of the particles formed is identical to the composition of the vapor in the bubbles, without phase separation.

Electrochemical methods have also been used for the production of maghemite nanoparticles [60]. The electrochemical synthesis of nanoparticles of  $\gamma$ -Fe<sub>2</sub>O<sub>3</sub> was performed in an organic medium. The size was directly controlled by the imposed current density, and the resulting particles were stabilized as a colloidal suspension by use of cationic surfactants. The size distribution of the particles was narrow, with average sizes varying from 3 to 8 nm.

### 3.2.2. Aerosol and Vapor Methods

Spray and laser pyrolysis have been shown to be excellent techniques for direct and continuous production of well-defined magnetic nanoparticles with exhaustive control on experimental conditions. Their high production rate can hold a promising future for magnetic nanoparticles useful for *in vivo* and *in vitro* applications. The main difference between spray and laser pyrolysis is in the final state of the ultrafine particles. In spray pyrolysis, the ultrafine particles are usually aggregated into larger particles, while in laser pyrolysis, the ultrafine particles are less aggregated due to the shorter reaction time.

**3.2.2.1. Spray pyrolysis** Spray pyrolysis is a process in which a solid is obtained by spraying a solution into a series of reactors where the aerosol droplets undergo evaporation of solvent and solute condenses within the droplet, followed by drying and thermolysis of the precipitated particles at higher temperature [61]. This procedure gives rise to microporous solids, which finally sinter to form dense particles.

This method represents a convenient procedure for obtaining finely dispersed particles of predictable shape, size, and variable composition. The resulting powders generally consist of spherical particles, the final diameter of which can be predetermined from that of the original droplets. The method offers certain advantages over other more commonly used techniques (such as precipitation from homogeneous solution) as it is simple, rapid, and continuous. Recently, this method has been used for the production of mesoporous microspheres [62] and phosphorescent nanoparticles [63].

Most of the pyrolysis-based processes employed to produce maghemite nanoparticles start with an Fe<sup>3+</sup> salt and some organic compound that acts as a reducing agent. It was shown that in this procedure, Fe<sup>3+</sup> is partially reduced to a mixture of Fe<sup>2+</sup> and Fe<sup>3+</sup> in the presence of organic compounds with the formation of magnetite, which is finally oxidized to maghemite. In absence of a reducing agent, hematite is formed instead of maghemite [64].

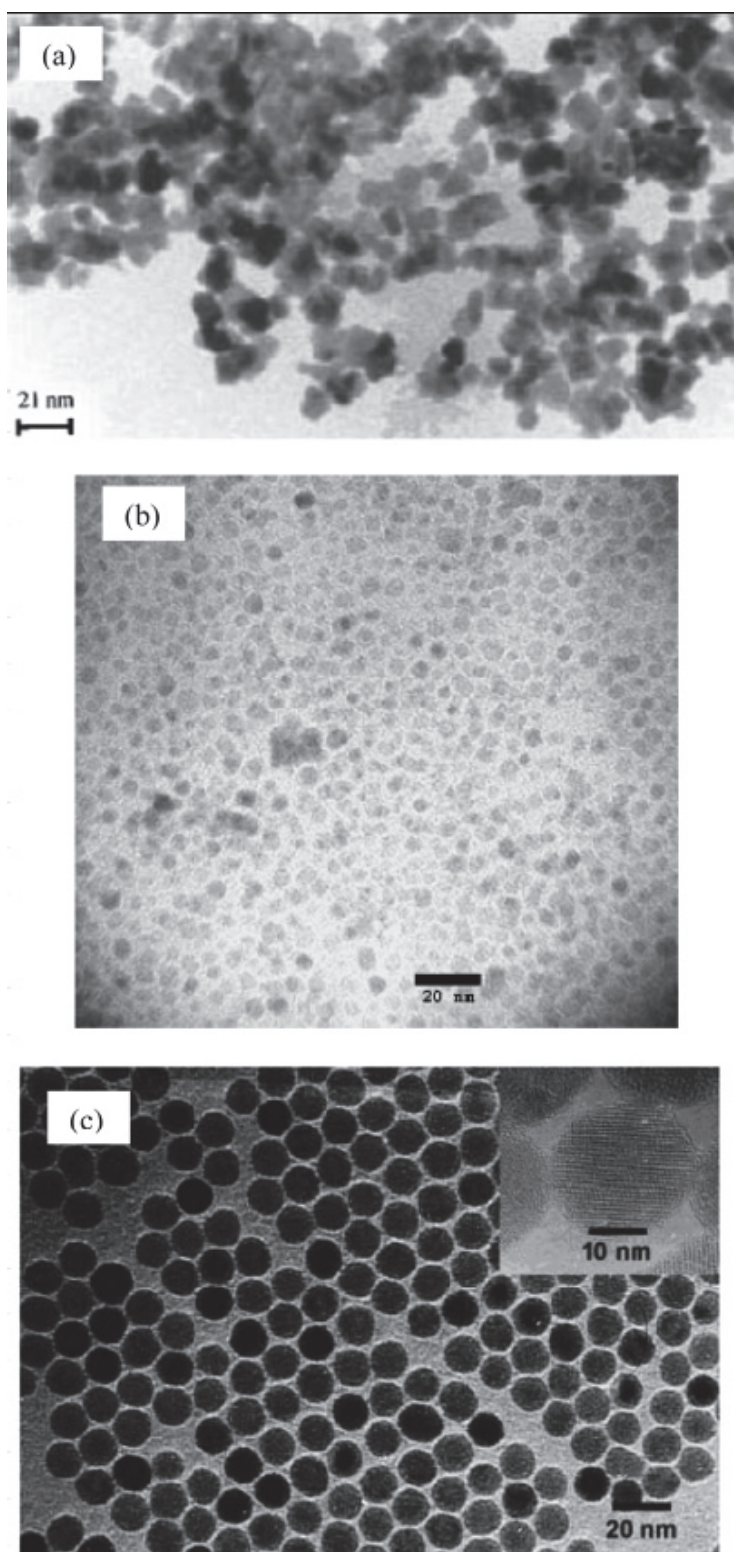


Figure 2: Magnetic nanoparticles prepared in solution by (a) the microemulsion method (maghemite), Reprinted with permission from ref: [38], copyright 1997, American Chemical Society (b) the polyol method (magnetite), Reprinted with permission from ref: [50], copyright at American Scientific Publishers and (c) high-temperature decomposition of  $\text{Fe(CO)}_5$  (maghemite), Reprinted with permission from ref: [53], copyright 2001, American Chemical Society. This entire figure appeared in author's review article, ref [126].

In alcoholic solutions, uniform  $\gamma\text{-Fe}_2\text{O}_3$  particles can be prepared with a wide variety of particle morphology and sizes, ranging from 5 to 60 nm, depending on the nature of the iron precursor salt [65]. A detailed description of the device used for this kind of synthesis can be found in the literature [66]. The device essentially consists of an aerosol droplet generator (atomizer, ultrasonic, etc.), a furnace, and a particle recovery system. Dense aggregates of spherical shapes composed of  $\gamma\text{-Fe}_2\text{O}_3$  subunits with mean diameters of 6 and 60 nm have been obtained using Fe (III) nitrate and Fe (III) chloride solutions, respectively. On the other hand,  $\gamma\text{-Fe}_2\text{O}_3$  obtained from acetylacetonate solution resulted in monodispersed particles of about 5 nm in diameter, while maghemite particles derived from Fe(II) ammonium citrate appeared as hollow spheres with a mean diameter of 300 nm. The latter consisted of small crystallites aggregated to form a shell, the size of which varied between 10 and 40 nm, depending on the heating temperature of the furnace.

**3.2.2.2. Laser pyrolysis** Since the pioneering work of Cannon and coworkers [67] on the continuous production of nanometer-sized powders by laser-induced processes, different powders such as Si, SiC,  $\text{Si}_3\text{N}_4$ , and Si-C-N composite have been prepared under a variety of conditions with sizes ranging from 5 to 20 nm [67, 68]. The method involves heating a flowing mixture of gases with a continuous-wave carbon dioxide laser, which initiates and sustains a chemical reaction. Above certain pressure and laser power, a critical concentration of nuclei is reached in the reaction zone, which leads to the homogeneous nucleation of particles that are further transported to a filter by an inert gas.

Pure, well-crystallized, and uniform  $\gamma\text{-Fe}_2\text{O}_3$  nanoparticles can be obtained in one single step by a  $\text{CO}_2$  laser pyrolysis method. Samples with particles of sizes as small as 3.5 and 5 nm and very narrow size distribution have been obtained under different experimental conditions [69, 70]. The device consists of a small reaction zone defined by the overlap of the vertical reactant gas stream and horizontal laser beam. The reaction zone, being safely separated from chamber walls, offers an ideal environment for the nucleation of small nanoparticles, with less contamination and narrower size distribution than that of conventional thermal methods.

To obtain  $\gamma\text{-Fe}_2\text{O}_3$  nanoparticles,  $\text{Fe}(\text{CO})_5$  was used as a precursor. Due to the fact that this precursor does not absorb radiation at laser wavelength ( $10.60 \pm 0.05 \mu\text{m}$ ), ethylene was used as the absorbent as well as carrier to transport the carbonyl vapor to the reaction zone. Ethylene does not decompose at the energy density used ( $652 \text{ Wcm}^{-2}$ ) but simply absorbs the laser radiation to heat up  $\text{Fe}(\text{CO})_5$ , which decomposes into iron and carbon monoxide. In order to obtain iron oxide, air needs to be introduced into the system, either with  $\text{Fe}(\text{CO})_5$  vapor causing oxidation under laser radiation or mixed with argon.

## 4. Cellulosic Nanofibers

### 4.1. Natural Occurrence

Natural fibers are pervasive throughout the world in plants such as grasses, seeds, stalks, and woody vegetation. They are also referred to as cellulosic fibers. Agricultural and forest wastes are made up of cellulosic fibers, which can serve as an excellent adsorption substrate to treat polluted water – a concept of ‘using waste to treat waste’. The cost of adsorption material for water treatment can hence be dramatically reduced, while other advantages include natural abundance, high mechanical strength, low energy consumption, low density and wide varieties. Coffee husk [71], peanut shells [72], bagasse [73], rice husk [74] and sawdust [75] has already been used as an adsorbent for wastewater treatment.

Wood fibers, the most abundant biomass resource on earth, are hollow tubes made up of cellulose embedded in a matrix of hemicellulose and lignin. Most of the cell-wall materials are located in the second layer, which consists of a helically wound framework of microfibrils (Figure 3) [76].

Reducing the size of cellulosic fibers to its constituent nanofibrils and nanowhiskers may elevate the overall cost, but may prove to be beneficial, performance wise. However this area is not so well-explored as far as water treatment application is concerned.

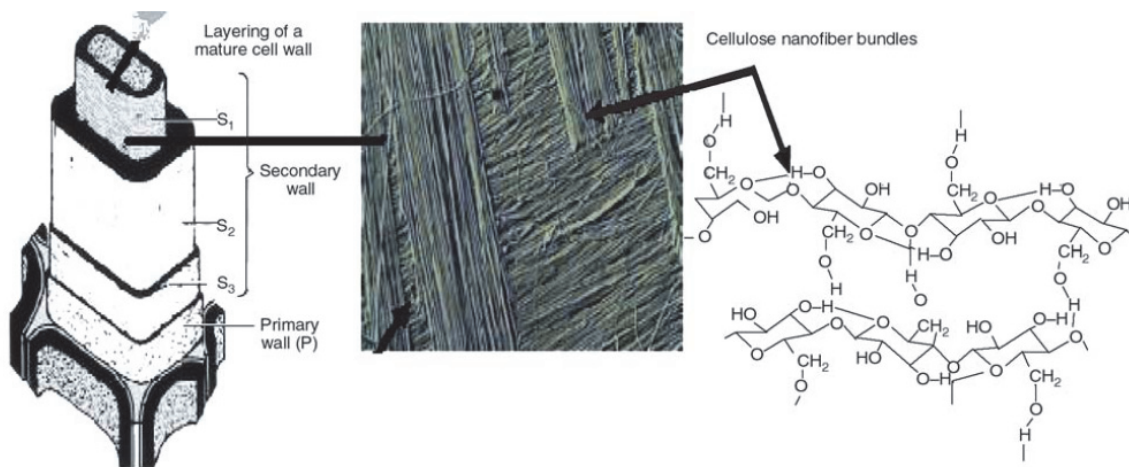


Figure 3: Microstructure of wood fiber cell wall:  $S_1$ ,  $S_2$  and  $S_3$  are the inner, middle and outer layers of the secondary wall, respectively, Adapted by permission from Macmillan Publishers Ltd. ref: [76]

## 4.2. Processing Techniques

### 4.2.1. Mechanical fibrillation

The fibrillation of pulp fiber to obtain nano-scale unit structures, called microfibrillated cellulose, is obtained through mechanical treatment of pulp fibers – a combination of refining and high pressure homogenizing processes. The refining process is common in the paper industry, and is done by an equipment called refiner. In a disk refiner, the dilute fiber suspension is forcefully allowed to go through a gap between the rotor and stator disks, which have surfaces fitted with bars and grooves, against which the fibers are subjected to repeated cyclic stresses. This mechanical treatment brings about irreversible changes in the fibers, increasing their bonding potential by modification of their morphology and size. In the homogenization process, dilute slurries of cellulose fibers previously treated by refining, are pumped at high pressure and fed through a spring high pressure loaded valve assembly. As this valve opens and closes in rapid succession, the fibers are subjected to a large pressure drop with shearing and impact forces. The combination of these forces promotes a high degree of microfibrillation in the cellulose fibers, resulting in microfibrillated cellulose [77].

The refining process is carried out prior to homogenization due to the fact that refining produces external fibrillation of fibers by gradually peeling off the external cell wall layers ( $P$  and  $S_1$  layers) and exposing the  $S_2$  layer and also causes internal fibrillation that loosens the fiber wall, preparing the pulp fibers for subsequent homogenization treatment [78].

### 4.2.2. Electrospinning

Electrospinning has been recognized as an efficient technique for the fabrication of polymer nanofibers. Various polymers have been successfully electrospun into ultrafine fibers e.g. cellulose acetate. There are basically three components in the instrument: a high voltage supplier, a capillary tube with a pipette or needle of small diameter, and a metal collecting screen. In the electrospinning process a high voltage is used to create an electrically charged jet of polymer solution or melt out of the pipette. Before reaching the collecting screen, the solution jet evaporates, and is collected as an interconnected web of small fibers [79, 80]. One electrode is placed into the spinning solution/melt, the other is attached to the collector. The electric field is applied to the end of the capillary tube that contains the solution fluid held by its surface tension. This induces a charge on the surface of the liquid. The potential difference depends on the properties of the spinning solution, such as polymer molecular weight and viscosity. When the distance between the spinneret and the collecting device is short, spun fibers tend to stick to the collecting device as well as to each other, due to incomplete solvent evaporation. Mutual charge repulsion and contraction of surface charges to the counter electrode cause a force directly opposite to the surface tension [81]. As the intensity of the electric field is increased, the hemispherical surface of the fluid at the tip of the capillary tube elongates to form a conical shape, known as the Taylor cone [82]. By further increasing the electric field, a critical value is attained when the repulsive electrostatic force overcomes the surface tension and the charged jet of the fluid is ejected from the tip of the ‘Taylor Cone’ [83]. The discharged polymer solution jet undergoes an instability and elongation process, which allows the jet to become very long and thin. Meanwhile, the solvent evaporates, leaving behind a charged polymer fiber (Figure 4). In case of polymer melts, the same process is performed, but under vacuum.

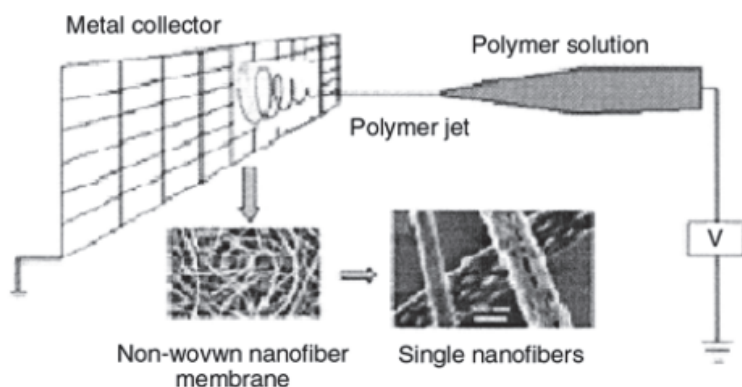


Figure 4: Schematic diagram to show polymer nanofibers by electrospinning, ref: [83]

### 4.2.3. Swelled precursor

Microcrystalline cellulose can be swelled and partly separated to whiskers by chemical and ultra sonication treatments. Dimethyl acetamide with 0.5 wt% LiCl solution can be used as a swelling agent. The microcrystalline cellulose (10wt%) in LiCl/dimethyl acetamide is agitated using a magnetic stirrer for 12 hours at 70°C, which causes the microcrystalline cellulose particles to swell. The slightly swelled particles are then sonicated in an ultrasonic bath for 3 hours over a period of 5 days with long intervals between each sonication treatment, to separate the cellulose nano whiskers [84].



#### 4.2.4. *Acid hydrolysis*

Suspensions of nanocrystalline cellulose can be prepared by acid hydrolysis. Hydrolysis is carried out in sulfuric acid with continuous stirring, immediately followed by 10-fold dilution with deionized water to quench the reaction. The suspension is then centrifuged at 6000 rpm for 10 min to concentrate the cellulose and to remove excess aqueous acid. The resultant precipitate should be rinsed, re-centrifuged, and dialyzed against water for 5 days until constant neutral pH [85].

#### 4.2.5. *By bacteria*

Nanofibrils of cellulose can be synthesized by some bacteria. For example, the cellulose produced by static cultivation of *Acetobacter xylinum*, sub species BPR2001, in a fructose/CSL medium at 30°C [86]. The bacteria is grown in a 400 ml Erlenmeyer flasks containing 100 ml of media. In order to remove the bacteria and to exchange remaining media, the produced cellulose pellicles are boiled in 1 M NaOH at 80°C for 1 hour followed by repetitive boiling in deionized water. To prevent drying and to avoid contamination, the washed cellulose is stored in diluted ethanol, in a refrigerator. The advantage of using bacterial cellulose lies in its high purity, fine fibrils (high surface area) [87], high tensile strength and water-holding capacity.

### 5. State-of-Art Applications

#### 5.1. *Magnetite*

Iron oxides have been reported to have a high affinity for the adsorption of arsenic and arsenate, due to the ability to form inner-sphere bidentate binuclear complexes with iron oxides [88, 89]. Magnetite nanoparticles have highest saturation magnetization of 90 emu/g among iron oxides. Therefore, magnetite nanoparticles can be used to adsorb arsenic ions followed by magnetic decantation.

#### 5.2. *Maghemite*

Tuutijärvi *et al.* [90] investigated the suitability of maghemite nanoparticles for As(V) adsorption and compared the As(V) adsorption efficiency of three different types of maghemite nanoparticle: commercially available (CM), home-made by mechanochemical method (MM) and home-made by sol-gel process (SM). They observed that the best As(V) adsorption capacity for all adsorbents were achieved at pH 3 and decreased gradually with increasing pH. MM possessed the highest As(V) adsorption capacity of these three maghemites, followed by SM and CM particles, which can be attributed to specific surface Areas, as MM particles has the highest surface area and CM particles the lowest. The adsorption maximum values based on surface area for all three maghemites were very similar, almost identical, which indicated that maximum As(V) adsorption capacity is related to surface area. This observation differs from the previous study [91], in which it was indicated that As(V) adsorption capacity is influenced by nanoparticle size rather than surface area.

Hu *et al.* [92] studied the removal and recovery of Cr(VI) from wastewater using maghemite nanoparticles. They noted that the adsorption reached equilibrium within 15 min and was independent of initial Cr concentration. The maximum adsorption occurred at pH 2.5. The adsorption data were analyzed and fitted well by Freundlich isotherm. Competition from common coexisting ions were negligible, which illustrated the selective adsorption of Cr(VI) from wastewater. Regeneration studies verified that the maghemite nanoparticles, which underwent six successive adsorption-desorption process, still retained the original metal removal capacity.

The adsorption data from Predescu *et al.* [93] indicated that good adsorption capacity for metal ion removal can be achieved by maghemite nanoparticles coupled with cationic resin ( $\gamma\text{-Fe}_2\text{O}_3\text{-R-H}$ ) and a higher adsorption tendency for hexavalent chromium in comparison with the other metal ions were observed.

### 5.3. nZVI

nZVI has become one of the most common adsorbents for the rapid removal of As(III) and As(V) in the subsurface environment [94-100]. Its application to remove varieties of pollutants has been demonstrated with halogenated hydrocarbons such as TCE, PCE [101-104], carbon tetrachloride [105], anions (e.g.,  $\text{NO}_3^-$ ,  $\text{Cr}_2\text{O}_7^{2-}$ ), heavy metals (e.g.  $\text{Ni}^{2+}$ ,  $\text{Hg}^{2+}$ ), radio-nuclides [106], As(III) [107] and organic compounds such as benzoic acid [108].

Kanel *et al.* [109] has characterized pristine nZVI as well as As(V)-treated nZVI materials. Their HR-TEM study confirmed the core-shell structure of pristine nZVI ( $\sim 20$  nm diameter core attributed to  $\text{Fe}^0$  and  $\sim 10$  nm thick shell due to iron oxide). Kanel *et al.* [109] has also carried out batch studies on the removal of As (Figure 5) with groundwater samples obtained from Bangladesh and West Bengal, India. The total iron concentration of groundwater from both sources were 10 mg/L. As(V) was spiked in both samples to obtain an initial As(V) concentration of 1 mg/L and its effect was studied using nZVI. As(V) was removed, with an efficiency reaching 100%, by 0.1, 0.2, and 0.4 g/L nZVI for the spiked DI water, Bangladesh groundwater and West Bengal groundwater samples, respectively. They proved that As (V) can be removed by adsorption/precipitation mechanism on nZVI (at neutral pH) in a relatively short time of only several minutes.

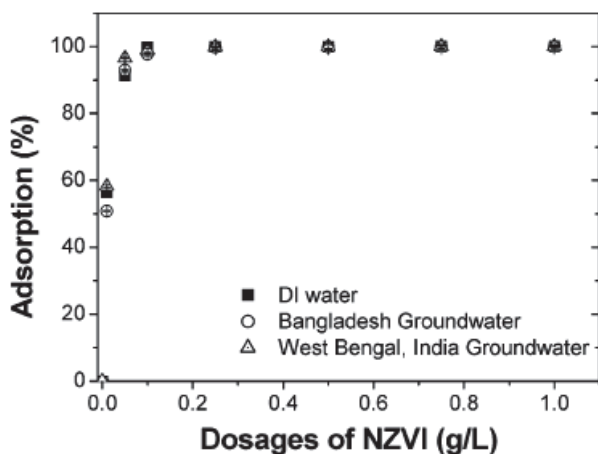


Figure 5: Sorption of As(V) on nZVI for spiked DI water with As (V): 1 mg/L in 0.01MNaCl, Bangladesh groundwater and West Bengal (India) groundwater samples; in all cases nZVI: 0.1 g/L, pH 7, 25 °C. Reprinted with permission from ref: [109], copyright 2006, American Chemical Society

### 5.4. Mixed oxides

Oxidation of magnetite results in reduction of saturation magnetization. However replacement of  $\text{Fe}^{2+}$  in  $\text{Fe}_3\text{O}_4$  by a small amount of  $\text{Co}^{2+}$  or  $\text{Ni}^{2+}$  can improve the oxidation resistance of the compound [110]. Oxidation resistance is an important factor for arsenic removal under atmospheric conditions. Hai *et al.* has studied arsenic adsorption ability of  $\text{Fe}_{1-x}\text{Co}_x\text{Fe}_2\text{O}_4$  (Co-ferrites) and  $\text{Fe}_{1-y}\text{Ni}_y\text{Fe}_2\text{O}_4$  (Niferrites) ( $x, y = 0, 0.05, 0.1, 0.2, 0.5$ ) nanoparticles [111]. For Co replacement, adsorption

did not change significantly when  $x < 0.1$  and reduced slightly when  $x > 0.1$ . However, the presence of Ni improved the adsorption to some extent (Figure 6).

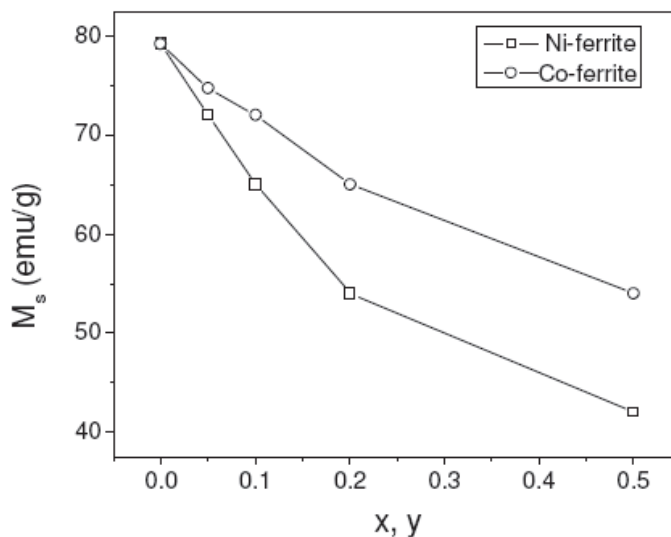


Figure 6: Saturation magnetization of the Co- and Ni-ferrite as a function of  $Co^{2+}$  ( $x$ ) and  $Ni^{2+}$  ( $y$ ) content, ref: [111]

### 5.5. Organic-inorganic nanohybrids

Literature shows [112] magnetic hydroxyapatite, made of hydroxyapatite (HAP) and  $Fe_3O_4$  nanoparticles, can adsorb 90% phenol in wastewater. Hydroxyapatite is chemically similar to bones and hard tissues in mammals and is one of the few materials classified as bioactive for biomaterial application. This unique magnetic sorbent has the capacity to regenerate after reaching adsorption saturation using ethanol as eluant and external magnetic field as separation unit. The efficiency of adsorption is reduced only by 10% over a six time use period. Besides, Tural [113] reported that glucamine modified magnetic sorbent has the ability to separate and preconcentrate boron.

Carbon nanotubes (CNT) due to their unique structures and exceptional properties have been the focus of research and development since their discovery in 1991 [114]. Their thermal and chemical stabilities have made them attractive adsorbents for organic and inorganic contaminants in water [115,116]. Peng *et al.* [117] prepared iron oxide - CNT magnetic composites and used for removal of Pb(II) and Cu(II) from water. They showed that after adsorption, the adsorbent could be separated from the medium by a simple magnetic process with >98% recovery. While CNT itself is a poor adsorbent for As(V), Poinern *et al.* [118] has reported that CNT-ferrihydrite composite can serve as an excellent adsorbent in arsenic removal. Their FESEM images show that the composite is made of regular CNT tubes of length < 2  $\mu m$  and outer diameter 30-50 nm, which is coated with agglomerated ferrihydrite particles in a bundle-like structure (Figure 7) and that surface area of the composite is almost double as that of CNT.



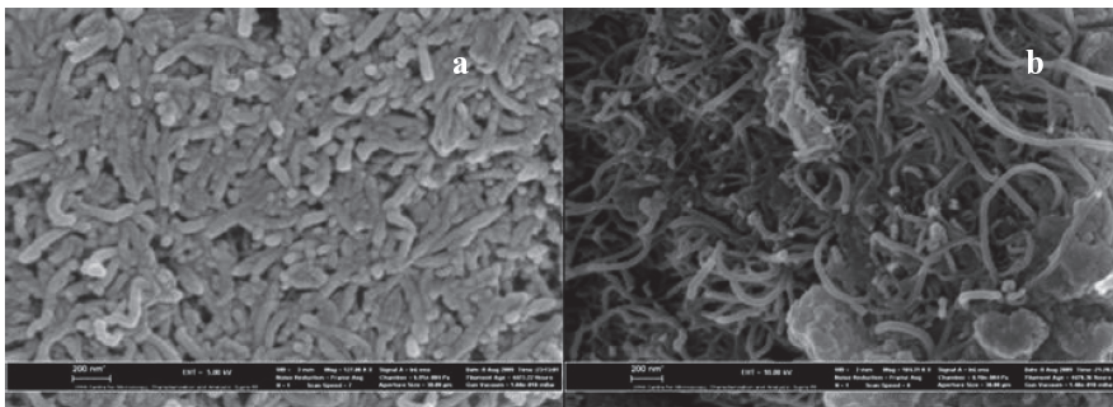


Figure 7: FESEM images of (a) CNT and (b) CNT-ferrihydrite composite, ref: [118]

### 5.6. Cellulosic biomass

Mahesh *et al.* [119] has studied the use of cost effective and ecofriendly plant cellulose based adsorbents, as an alternative and effective substitute of activated carbon, for the removal of toxic dyes from waste water, namely the use of sugarcane baggase, pretreated with formaldehyde (referred as raw baggase) and sulphuric acid (referred as chemically activated baggase), for the removal of crystal violet dye from simulated waste water; the raw baggase showing better adsorption efficiency.

Asandei *et al.* [120] have shown the effectiveness of lead (II) ion removal from aqueous solution of chitosan being mainly dependent on the initial concentration of lead (II) ions to chitosan dosage ratio, which should be optimized by a compromise between the removal yield and cost-effectiveness of the process. Their adsorption data well-fitted Langmuir isotherm.

Igwe *et al.* [121] reported enhanced adsorption capacity of EDTA modified maize husk due to the chelating effect of ethylenediamine tetra acetic acid (EDTA) while studying Cd(II), Pb(II) and Zn(II) ion removal from wastewater.

The nonwoven webs of fibers produced from the electrospinning process have high specific surface areas, nano scale pore sizes, high and controllable porosity and extreme flexibility with regard to the materials used and modification of the surface chemistry of the fibers. Desai *et al.* reported the electrospinning difficulties of chitosan/poly (acrylamide) and overcame these by varying the parameters such as polymer concentration and temperature and thereby uniform beadless nanofibers were achieved. In another work, potential use of electrospun chitosan/poly(ethylene oxide) (PEO) nanofibers for heavy metal ion binding, antimicrobial as well as physical separations were clearly examined. They also proved that filtration efficiency was strongly related to the size of the electrospun fibers and percentage of the chitosan present on the surface. They have utilized these membranes in binding hexavalent chromium ions [122-124].

A company named Elmarco s.r.o. has successfully implemented the nozzle-less electrospinning technology (Nanospider™) to produce cellulosic nanofibers for air filtration and other applications.

## 6. Nanotechnological Principal applied to Water Purification

The principle behind application of magnetic nanoparticles and cellulosic nanofibers for heavy metal removal from water, is the theory of adsorption, which can be found in several textbooks of physical